Enhancement of NiTi alloys biocompatibility and corrosion resistance by thermal treatments

G. Mealha[1], T. M. Silva[1,2], J. C. S. Fernandes[1]

[1]CQE, Instituto Superior Técnico, Universidade de Lisboa, Portugal
[2]ADEM, GIMOSM, Instituto Superior de Engenharia de Lisboa- ISEL, Portugal

December 2016

Abstract

Nitinol (NiTi) is a nearly equiatomic nickel-titanium alloy, which is suitable for biomedical applications due to its unique mechanical properties (such as shape-memory effect and superelasticity) and high corrosion resistance and biocompatibility. Despite this, the high nickel content is considered a great problem of this alloy, being known reports of inflammatory and allergic processes caused by the release of nickel ions from NiTi devices. In the present work, thermal treatments were performed in the surface of Nitinol in two types of environment (air and nitrogen) and at two different temperatures (250 °C and 350 °C). Corrosion resistance of the treated alloys was analyzed through electrochemical techniques in Hank's solution at 37 °C (to simulate physiological conditions) and the results were compared with untreated Nitinol. The modified surfaces were characterized by X-ray photoelectron spectroscopy (XPS) and Auger electron spectroscopy (AES). The performed surface treatments proved to influence the electrochemical behaviour of Nitinol. From EIS spectra, and by fitting the data to an equivalent circuit, a duplex structure was proposed to the alloys oxide film, composed by an inner compact layer and an outer porous layer. Results from the surface analysis concluded that the nickel content was substantially decreased in the outermost surface layers, especially when treated at 350 °C in N_2-controlled environment.

Keywords: Nitinol, biomaterials, corrosion, thermal treatments, oxide film

1. Introduction

Shape-Memory Alloys (SMA) is a group of materials that have been largely applied in the production of biomedical devices in the last years, in particular for minimal invasive techniques [17], due to their capability to recovering the original shape and dimensions after large deformations. The most used SMA is Nitinol (NiTi), a nearly equiatomic nickel-titanium alloy, characterized by its superelasticity, relatively stable cyclic performance, good workability and good resistance to corrosion and fatigue.
NiTi's shape-memory effect (SME) is a consequence of a solid state phase change between two different structures, austenite (rigid) and martensite (malleable), called martensitic transformation. This can be defined as a displacive, diffusionless transformation where a new phase is obtained, through an atomic reordering at short distances, having both phases the same chemical composition. Figure 1 shows a scheme of the SME in Nitinol. Cooling the high-temperature phase, austenite, will provoke a change in its crystal structure, when a certain M_s temperature (martensite start temperature) is reached; as temperature continues to fall, the transformation to a martensitic structure proceeds until M_f temperature (martensite finish temperature), at which the specimen is 100 % martensite.

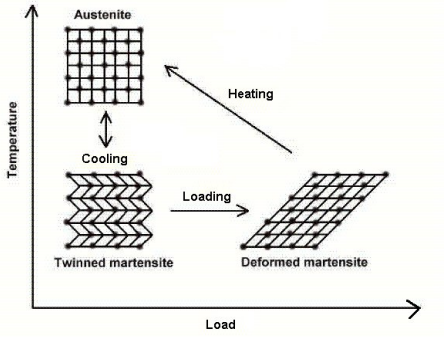

Figure 1: SME in Nitinol.

In order to obtain the original material, with the same initial shape and dimensions, the material in the martensitic state is heated, and the austenitic structure begins to form at a temperature named A_s (austenite start temperature), being fully transformed at A_f (austenite finish temperature). This

ability of being easily shaped at low temperatures, allowing the material to change to a totally different form at an higher temperature, is of extremely importance for the application of NiTi alloys.
Martensitic transformation can also be induced by means of an applied stress, at a constant temperature $T > A_f$, showing a mechanical behaviour called *superelasticity*: through the application of strains above a certain magnitude, stressed detwinned marteniste is obtained; by totally removing the stress, the material returns to its initial austenitic state, with a net deformation after the load-unload cycle being zero.
Another mechanical property of NiTi of great interest is related with its Young's modulus, being very close to that of cortical bone (in the range of 30–50 and 10–30 GPa, respectively) when compared with other metallic materials used in medical implants [6]. In this way, implants made of 316L stainless steel, Ti- or CoCrMo- alloys, by having very high Young's modulus will bear almost all the subjected load, leading to negative effects for the bones around the implant site (in a phenomenon called *stress shielding effect*) [6].
Apart these unique properties, there are some concerns that may arise from the use of NiTi devices, due to the considerable amount of Ni on its composition ($\simeq$ 55 % wt); the presence of this toxic and carcinogenic element may affect two crucial requirements of a biomedical material: excellent biocompatibility (in order to not cause harmful effects in the host body) and high resistance to corrosion (to avoid material's deterioration due to chemical interactions with the environment).
In vitro and *in vivo* studies on biocompatibility of NiTi alloys had been made since the late 1970s, with a tremendous boom in the last 25 years. In a work performed by Assad et al. [3], NiTi and CP-titanium presented less genotoxic results to metaphase chromosomes than 316L stainless steel, with the cell culture response in the presence of NiTi being satisfactory. Using murine fibroblast and osteoblast cell lines, no cytotoxicity was detected in the direct-contact evolution testing [16]; in that work, NiTi was considered a novel and promising biomedical material to be used in the future.
In respect to *in vivo* experiments, there are some conflicting results, in which arise some concerns with this alloy, such as inferior properties (like low bone contact) compared with stainless steel, Co- and Ti - alloys [5, 20], or a high nickel concentration in the blood [13].
In addition to *in vitro* and *in vivo* reports, NiTi has also been used as human implant material either for hard and soft tissue, with results that conclude that NiTi presents good potential for its clinical use [10]. However, due to a clear lack of knowledge about Nitinols biocompatibility, its medical applications have been hindered worldwide [6] and the number of trials is quite scarce, what makes it harder to reach an agreement about this matter.
In terms of corrosion resistance from NiTi alloys, it relies on the presence of a passive oxide film that covers its surface and inhibits the development of uniform corrosion. Nitinol becomes protected from aggressive physiological environments due to the formation of a Ti-enriched oxide layer with low amounts of nickel, which is in contact with a Ni-enriched sub-layer; the big amount of nickel present in this sub-layer is responsible for turning NiTi resistance against passivity breakdown much poorer when compared with pure titanium, resulting in the onset of pitting corrosion. Ni cations are released from the Ni-enriched sub-layer through pores in the outermost TiO_2 film, with possible hazardous consequences due to the adverse effects associated with Ni^{2+} species, as material's degradation proceeds [11]. The preferential TiO_2 film formation is corroborated by thermodynamic data, through the analysis of Gibbs free energy (ΔG) values. ΔG of a reaction gives a measure of the driving force that makes that reaction to occur: a negative value indicates that the reaction can proceed spontaneously without external inputs, while a positive value indicates that it will not. At 25°C, free energy of formation for TiO_2, TiO and NiO is, respectively, -889.5, -495 and -211.7 kJ mol^{-1}, what seems to favour the formation of titanium dioxide over other possible oxides [18].
In the last 15 years, several studies concerning the corrosion resistance of NiTi have been conducted; Stepan et al. [19] developed a prosthetic heart valve using thin NiTi film and tested under *in vitro* and *in vivo* conditions (by implantation in pigs using stents) and assigned very good suitability for clinical applications. In another study [12], NiTi experienced corrosion in aggressive environments. Most of the experiments show promising results, with some authors highlighting the importance of performing more complete tests, through longer periods and by subjecting the samples to loading/unloading situations, due to the complex working conditions inside the human body. In this way, dynamic tests are also very important to perform, caused by differences in the corrosion behaviour from stressed and untressed samples [8]
In order to obtain better performances for NiTi, several treatments may be considered, through the development of coatings and surface modifications. One approach can be to promote the formation of oxide films by taking advantage of the high oxygen affinity of titanium, by anodization processes or thermal oxidation [22]. Improvements also can be achieved by depositing materials on NiTi's sub-

strate, obtaining a coating between the alloy and the surrounding environment; in this way, calcium-phosphate based compounds, such as hydroxyapatite, proved to have exciting results [23].
Nitinol, for being the most used SMA, due to its unique mechanical properties, has been exploited through the years in many different fields, as orthodontic archwires, vascular stents and orthopedic devices, among other forms. The self-expandable stents, by providing minimally invasive treatments instead of major surgeries, are probably the most successful NiTi devices, with especial application in cardiovascular surgery, but also in gastrointestinal and urological applications. In situations of coronary heart diseases, in which there is a narrowing of the blood vessels, a filter is inserted as a straight thin wire via a small bore catheter; upon reaching the interior of the blocked artery and sensing its body temperature, and making use of the shape-memory effect, the stent reverts to its complex filter shape and locks into place permanently, trapping any further stenosis.
Another common application is in the orthodontic field, as archwires. The successful use of NiTi relies on its ability to apply to the teeth almost constant forces, and low in magnitude, during dental repositioning, obtained as a consequence of the bone-remodeling process, due to the alloy's extended elastic domain, which allows it to recover from large deformations. In this way, the device induces physiological dental movements without damaging the underlying tissues and causing minimal discomfort to the patient, as opposed to other classic materials that by applying discontinuous forces can cause hyalinization, a deleterious process caused by tissue disintegration; as a consequence of such a high biological and clinical effectiveness of NiTi wires, the frequency of readjustments by the attending orthondist drops from every month (the interval usually needed for retensioning stainless steel wires) to a few times per year, and with a pain decrease during the entire treatment period [4].

2. Experimental

2.1. Materials

A rod-shaped NiTi alloy with 8.509 mm of diameter, designated as alloy B and supplied by *Memory-Metalle GmbH*, was cut in disks with 6 mm of thickness (approximately) and polished up to 2400 grit SiC paper and then with 1 μm diamond paste (from *microdiamant*). After polishing, the specimens were cleaned in 2-propanol through an ultrasonic bath (*Branson 1200 Ultrasonic Cleaner*) to remove any left impurity.
The metallic pieces subjcted to thermal treatment were sent to Polytechnic Institute of Setbal (IPS) to perform the surfaces modification in a tubular furnace, in two types of atmosphere (air and nitrogen) at two different temperatures (250 and 350 °C). Before the electrochemical tests, each specimen was covered with a beewax and colophony resin mixture, except for an window corresponding to the area to be tested.

2.2. Electrochemical studies

The electrochemical measurements were performed in a 3-electrode cell, composed by the sample understudy (the *working* electrode), a *Saturated Calomel Electrode* (reference electrode) and a Pt coil acting as *counter-electrode*. The cell was introduzed in a Faraday cage, with the solution contained in the cell kept at 37 °C (to simulate the human body temperature) through a thermostatic bath system with natural aeration. The tests were conducted using two different physiological solutions: Hank's and PBS, with the last one being only used for the potentiodynamic polarization curves of untreated Nitinol.

2.3. OCP and Anodic Polarization measurements

The samples were immersed in physiological solution at open circuit potential for two hours (one hour for the untreated NiTi). To obtain the polarization curves, a potential scan was performed starting from 20 mV below E_{corr} upward to 1.5 V/ECS, with a scan rate of 1 mV/s. For that, a potentiostat from *Gamry Instruments*, *Reference 600* was used, coupled to a computer and through DC105 software.

2.4. EIS

The electrochemical impedance spectroscopy (EIS) trials were performed using the EIS300 software, from *Gamry Instruments*, controlled by a computer. The measurements were taken after stabilization of the OCP and by imposing a sinusoidal perturbation, through an AC voltage perturbation of 10 mV rms, from 100 kHz to 10 mHz. Successive spectra were acquired through time, until the stabilization of the system. Nyquist and Bode plots were obtained using a dedicated software, ZView®, from *Scribner Associates*.

2.5. Surface Analysis Techniques

Two techniques were used to evaluate the surface of NiTi alloys: X-ray Photoelectron Spectroscopy (XPS) and Auger Electron Spectroscopy (AES). Both analysis were performed using a Microlab 310F from *Fisons Instruments* (*VG Scientific*), a field-emission Auger microprobe. XPS spectra were acquired in CAE mode, using an Mg non-monochromated anode as X-ray source, and working at an energy of 15 keV. In AES, the concentration profiles were obtained by means of a Ar^+ beam of high purity, at the energy of 1 keV, $1x10^{-7}$ mBar of pressure and with a current density range of 0.5-

0.6 μA/mm^2; the Auger spectra was acquired in CRR mode using an energy of 10 keV and a current of 50 nA (approximately) for the electron beam.

3. Results and discussion

3.1. OCP and anodic polarization curves for untreated NiTi

The corrosion behaviour of non-modified Nitinol was evaluated and compared in two physiological solutions. The values of the stabilized E_{corr} obtained for Hank's and PBS were -0.342 and -0.343 V, respectively, indication of a similar corrosion behaviour of NiTi in both electrolytes. The OCP measurements show a discrete trend to reach more positive values, enhancing the passive behaviour of the material. This meets with data presented by Andreeva [2] in a 1964 report, in which a titanium oxide film formed in air (at room temperature) was steadily grown from a thickness of around 1 nm to 25 nm total, over a period of 4 years.

Table 1 resumes the main parameters obtained from the anodic polarization curves; NiTi presents a similar behaviour in both environments, with a passive region plateau of 1 V approximately, indicating the presence of an oxide layer formed on the surface of the sample that prevents the advance of material degradation. According to published literature, the transpassive potentials for untreatd NiTi samples are normally in the range of 0.8-1.2 V [14], which is observed as result of these experiments (E_b of 1.046 and 1.023 V in Hank's and PBS respectively). The passive region, characterized by tiny variations of the current density with the increasing potential, ends with an abrupt increase of current values, what could be caused by pitting or crevice (resulting in localized corrosion), or by oxygen evolution due to oxidation of water; but in the present case is believed to be a consequence of oxygen evolution [21], as no corrosion evidences were found in any of the specimens, for both simulated environments.

Table 1: Anodic polarization curves parameters for untreated Nitinol.

Parameter	**Hank's**	**PBS**
$\mathbf{E_{corr}}$ **(V)**	- 0.342	- 0.343
$\mathbf{i_{pass}}$ **(μA/cm^2)**	2.62	2.83
$\mathbf{E_b}$ **(V)**	1.046	1.023
$\mathbf{E_b - E_{corr}}$ **(V)**	1.388	1.366

3.2. OCP and anodic polarization curves for modified NiTi

After NiTi corrosion behaviour had been analyzed in two different environments, the focus centered on trying to get better results by modifying the surface of the alloy, with the measurements being performed only in Hank's solution from now on; for that, some samples were subjected to thermal treatments, varying temperature and oxidation atmosphere, through four different surface modification types: oxidation in air and in nitrogen atmosphere, at 250 and 350 °C.

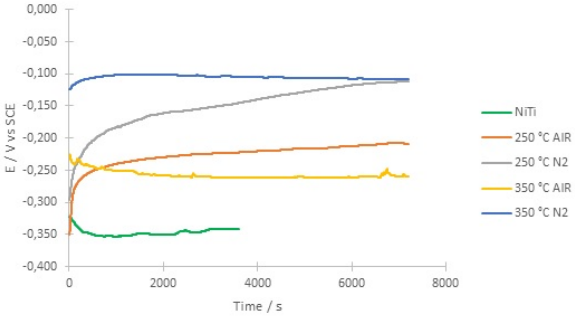

Figure 2: Open-circuit potential for thermally treated and untreated NiTi in Hank's solution at 37°C.

The open-circuit potential curves of the treated samples and the respective comparison with that of previous measured untreated NiTi are depicted in Figure 2. In general, the thermal treatments provoked a considerable increase of E_{corr}, with 3 different identified plateaus: under N_2, air atmosphere and raw NiTi. The increase of the potential values (in comparison with that of NiTi) is related with the presence of passive layers; the ones treated at 350 °C, more stable during the monitoring, and those at 250 °C, with an asymptotical increase in E_{corr}, indicating a continuous build-up of their oxide layer after immersion.

A stable value of around -0.110 V was reached for the N_2 treated Nitinol, while more negative values were obtained under air oxidation (-0.209 and -0.259 V at 250 and 350 °C, respectively) suggesting that treatments in N_2 atmosphere enhance NiTi corrosion resistance more than in air.

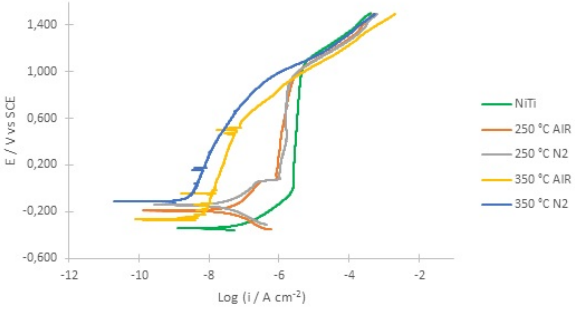

Figure 3: Anodic Polarization Curves for thermally treated and untreated NiTi immersed in Hank's solution at 37°C.

In the same manner as before, anodic polarization curves were obtained after the OCP measurement, being represented in fig. 3. The current densities observed for the treated NiTi are significantly lower than that of untreated ones, showing an improvement of the corrosion resistance. Furthermore, the current density at the passive region of the samples treated at 350 °C is substantially lower than for the others (in about two orders of magnitude), what is an indication of the enhanced protection conferred by the passive film formed under these conditions. With respect to the 250 °C samples, a more similar behaviour with the standard alloy is observed, with a visible passive region between 0.08 and 1.0 V; by this, it's plausible to assume that the protective character of the oxide film formed at 250 °C is slightly higher than the native film of NiTi but substantially lower than the ones treated at 350 °C.

3.3. Electrochemical Impedance Spectroscopy

EIS measurements were performed over a period of 1 week, in order to analyze with more detail the corrosion resistance of NiTi alloys and to get more specific informations about its formed passive layer. Figures 4-8 represent the typical Nyquist and Bode plots for the five different types of samples, with figure 4 corresponding to the untreated Nitinol.

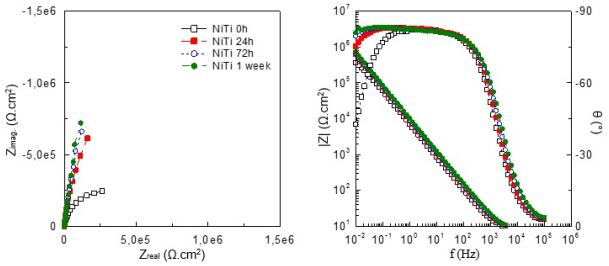

Figure 4: Nyquist and Bode plots of untreated NiTi.

In the case of the native material, it is possible to observe an enhancement of the corrosion resistance with time, with impedance values getting higher as the time goes on; this result is a consequence of a progressive improvement of the oxide's film protection on NiTi's surface.

The corrosion behaviour of the alloy turns to be substantially different with the thermal treatments. A common feature from all of them (figures 5-8) is related with the immediate corrosion resistance, with higher resistances and phase angles close to -90° over a wider frequency range (illustrating a near-capacitive response), for t = 0 h in comparison with untreated NiTi.

Among the subjected treatments, different behaviours on Nitinol's surface were obtained. Oxidation at 350 °C in N_2-controlled environment seems to be, by far, the most promising tested treatment, with high impedance values and a phase angle very close to -90° at medium and low frequencies, being independent from time (figure 5). Figures 6 and 7 illustrate also an enhancement in the corrosion resistance compared with untreated NiTi for t = 0h, for 350 °C in air and 250 °C under nitrogen environment, respectively (with the first having higher impedance values); although presenting a high resistance against corrosion, the protective behaviour of the formed passive films seems to be slightly decreasing over time.

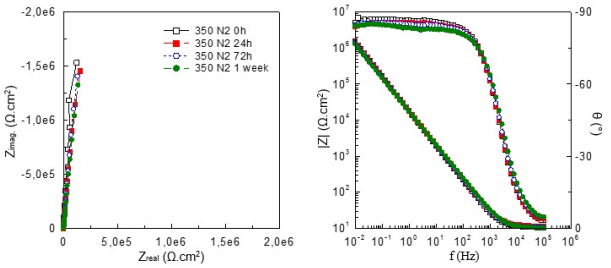

Figure 5: Nyquist and Bode plots of NiTi treated in N_2 environment at 350 °C.

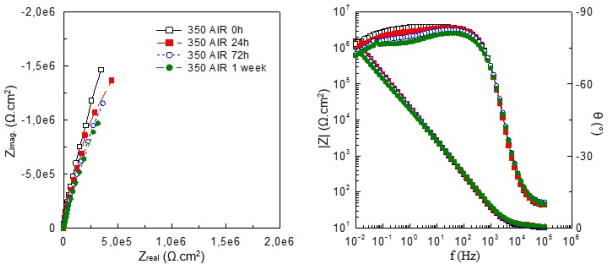

Figure 6: Nyquist and Bode plots of NiTi treated in air at 350 °C.

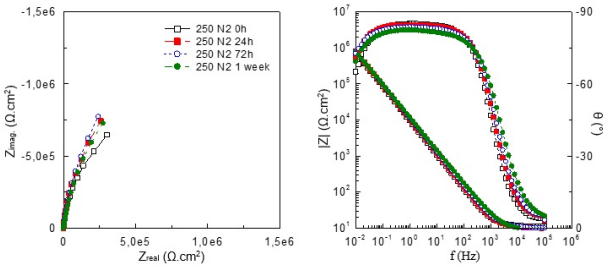

Figure 7: Nyquist and Bode plots of NiTi treated in N_2 environment at 250 °C.

Finally, impedance spectroscopy results indicate that one of the performed treatments does not improve the corrosion resistance of the alloy at a medium/long term. In spite of showing a slightly higher resistance against corrosion in the beginning of the experiment (in comparison with the untreated material), the oxide layer of NiTi treated in air at 250 °C loses quickly its protective character (figure 8).

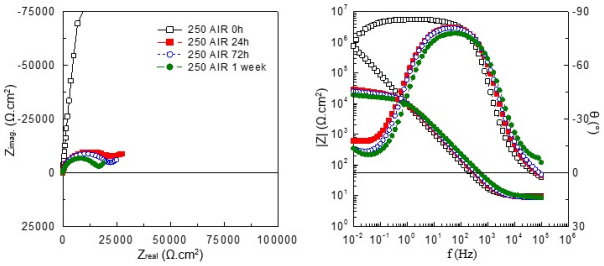

Figure 8: Nyquist and Bode plots of NiTi treated in air at 250 °C.

The concept of equivalent circuit means that an electrochemical process can be represented through an electrical model. By the analysis of the different plots obtained from EIS, a proposal to explain the structure of NiTi surface was suggested, represented in figure 9:

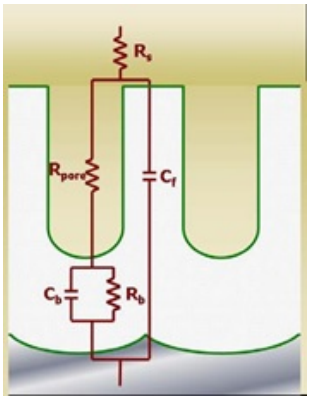

Figure 9: Proposed structure for the oxide film on NiTi and its equivalent circuit [9].

with the exposed equivalent circuit being constituted by three resistances - R_s, the solution resistance measured between the working and reference electrodes, R_{pore}, the additional resistance of the solution inside the pores, and R_b corresponding to the barrier layer resistance - and two capacitances, representing the barrier layer and the overall film in the porous walls. Constant phase elements (CPE) are used instead of pure capacitances in the fitting of EIS spectra to show the deviation from the ideal behaviour.
The model of figure 9 assumes a "duplex" structure for the oxide film on the surface of NiTi: an inner and dense barrier layer followed by a porous one. According to Mieluch [15], it is common to use a two-layer model, composed by an inner compact layer (acting as a barrier) and an outer porous one, when studying the oxide films on passive materials. In this model, it is possible to assume that the outer layer basically consists of the same oxide as the inner layer, but possesses microscopic pores which are filled by the surrounding solution.
Given this structure, the charge transfer can be conducted through two different ways:

- in pore direction, counting on the contributions of the electrolyte resistance inside the pores (R_{pore}) and the crossing of the thin barrier layer, characterized by its resistance and capacitance, R_b and C_b, respectively;
- crossing of the entire film thickness outside the pores, represented by it capacitance, C_f - the respective resistance is not represented because the flow of electrons is not expected to occur due to the very high resistance in parallel with the capacitance.

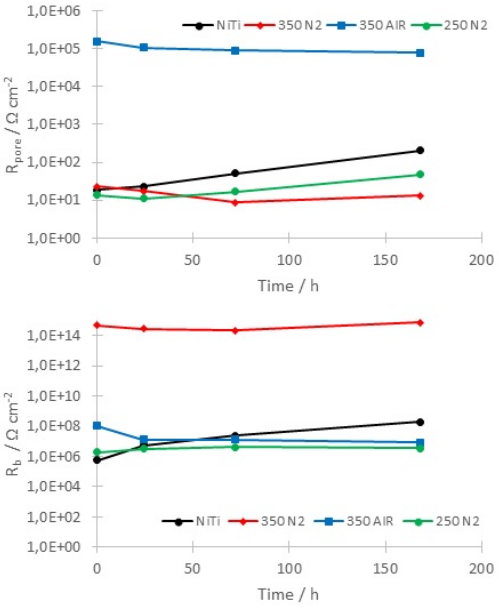

Figure 10: R_{pore} and R_b evolution through time.

Figures 10 and 11 show the results from the fitting of the EIS data with the duplex model, through the variation of the resistances R_{pore} and R_b and capacitances C_f and C_b along the experimental time, respectively; representation of NiTi treated in air at 250 °C was excluded due to the negative impedance results when compared with the untreated alloy.
The resistance and capacitance values of the native NiTi match with what was observed in the EIS spectrum, in which the corrosion resistance was improved through time. Both resistances substantially increase, while C_f and C_b decrease, although in a less pronounced way; assuming an oxide's film capacitance expressed by $C = \varepsilon\varepsilon_0 A/d$, being d the oxide thickness, A the surface area, ε_0 the absolute permittivity in vacuum and ε the oxide's dielectric constant (with a value around 100 [7]), the native alloy's behaviour can be explained as being due to

an increase of the porous and internal layer's thickness (since both capacitances decrease), enhancing the protective capacity of the material. A reduction in the pore's area (caused, for example, by pore's sealing) may also result in the same evolution.
The high corrosion resistance of the samples treated at 350 °C relies, according to figure 10, on different layers: while the treatment in N_2 produces very high values of R_b, with an average of $4.3x10^{14}$ Ω cm^2, the one treated in air shows high resistance in pore direction, comparing with the other samples; this last observation can be related with a small area from the pores, a big tortuosity of them (which relates to the low values of the respective n parameters, in the 0.5 - 0.7 range) or a considerable thickness of the outer layer. Both R_{pore} and R_b from 350 °C oxidation in air slightly decrease along the experiment, being in agreement with the slight loss of protection observed in fig. 6.

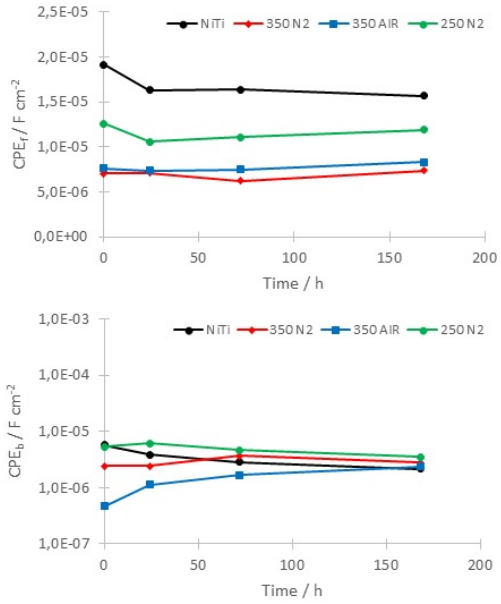

Figure 11: C_f and C_b evolution through time.

In terms of capacitances, the behaviour of all samples present a very similar trend, specially those related to the pores' wall, with almost no variation of C_f through time. In which concerns C_b, although with relatively different values at t = 0h, they tend to reach approximately the same values by the end of immersion. Moreover, almost no time evolution is observed for the samples treated in N_2, whereas a decrease of C_b is noticed for the untreated material (in line with the corresponding increase of R_b, as discussed above) and an increase of C_b is observed for the samples treated in air at 350 °C. In this last case, and as already discussed, tortuous pores may have been formed, leading to quite low initial values of capacitance and very high R_{pore} due to the long solution pathways, so the observed variations could be attributed to the degradation of that porous layer, with short-circuiting of the pores. It is important to stress that the present discussion refers to capacitances, although being based on the Y_0 values of the respective CPE's, as the respective n values are normally very close to 1 (between 0.90 and 0.96, with the exception for the $n(CPE_b)$ of 350 °C, which increases from 0.47 to 0.76, possibly a consequence of the high tortuosity of its oxide layer).

3.4. Surface analysis

The surface of the most-promising samples, in terms of corrosion resistance, the ones thermally treated at 350 °C, was analysed through XPS and AES and compared with the native passive layer of NiTI.
Naturally, some differences are expected to be noticed between each treated sample. The treatment in air atmosphere promotes (in theory) the oxidation of both constituents of the alloy (Ni and Ti), with the outer surface of NiTi being richer in Ti, due to its higher affinity to be oxidized. In this case, nickel is localized mostly in the metal/oxide interface or at the inner part of the oxide.
The use of an oxygen shortage atmosphere, such as the N_2 one, is expected to cause a selective oxidation of titanium atoms, having a protective oxide barrier mainly made of TiO_2, with the goal of avoiding the nickel presence in NiTi surface and its release to the surrounding environment.

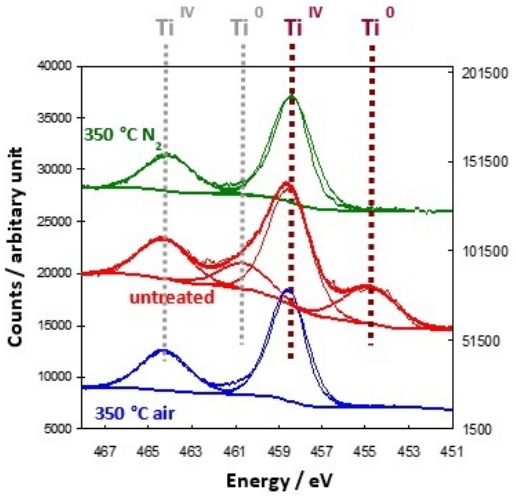

Figure 12: XPS spectrum in Ti 2p region for untreated and treated NiTi in air and N_2 environment at 350 °C.

The observation of the XPS spectra reveals the existence of Ti and Ni in the oxidised state (Ti^{IV} and Ni^{II} respectively) in the three different samples, indicating the presence of a protective oxide layer. Furthermore, the presence of the constituent

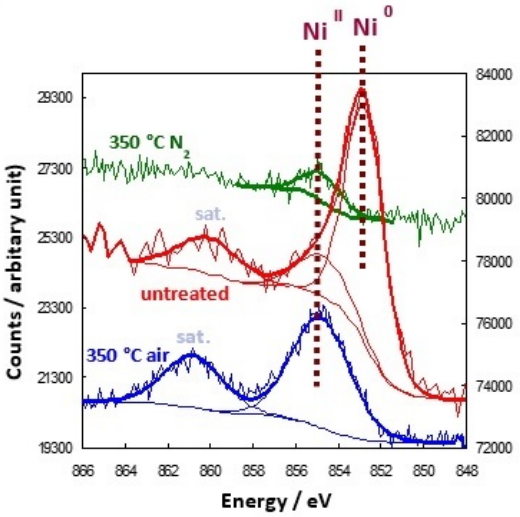

Figure 13: XPS spectrum in Ni 2p region for untreated and treated NiTi in air and N_2 environment at 350 °C.

elements in the metallic form (Ti^0 and Ni^0), is only detected in the case of untreated NiTi: although presenting a passive layer that confers stability to the alloy, that native film is very thin when compared with the treated samples.
As a result of the N_2-controlled environment treatment, the peak's area of Ti^{IV} is substantially bigger than that of Ni^0, meaning that the formed oxide layer is mostly made of TiO_2. In the other two cases, the area of the peaks of the oxidized elements are more similar, result of a bigger presence of nickel in the passive layer.

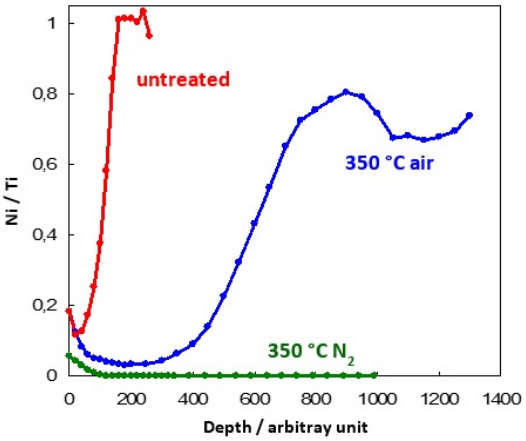

Figure 14: Evolution of Ni/Ti ratio along the worn depth for untreated and treated NiTi in air and N_2 environment at 350 °C.

The results of Auger Electron Spectroscopy are shown in figure 14. According to the Auger concentration profiles, it is possible to see that the Ni concentration is much lower than that of Ti in the three different samples surfaces, especially for the one treated in N_2 environment, which is approximately half of that for the other situations. The very similar value of Ni/Ti for the untreated and treated in air at 350 °C sample is related with the same oxide formation mechanism, being a result of the tendency of each element to form oxides and their respective diffusion coefficients.
Analogously of what was concluded from XPS results, the native's film thickness is found to be small, justified by the strong increase of Ni with the worn depth, reaching the ratio of 1 (corresponding to the alloy's substrate) for a relatively short depth. A sub-surface region very poor in nickel is detected as a result of oxidation in air; however, for more internal layers, the concentration of Ni starts to become more and more significant, although never reaching the same quantity than titanium. This means that the passive layer formed through this method is thicker than that of untreated NiTi, but not chemically constant in its composition.
The selective oxidation of NiTi in N_2 environment, in addition to having reduced the nickel concentration of the oxide layer surface, almost provokes an elimination of that element for all the examined depth; in case of corrosion, Ni ions release will be extremely minimized from the implant simply, because there is a lack of them in the outermost regions of the material. Titanium's preferential oxidation over nickel, enhanced in environments with low-oxygen concentration, can be explained by the tendency of formation of its oxides, with a substantially lower value of $\Delta G(TiO_2)$ when compared with $\Delta G(NiO)$, in a very wide temperature range [1].

4. Conclusions and future work

The corrosion behaviour of surface modified Nitinol was investigated in a simulated physiological solution through electrochemical measurements and compared with the untreated alloy. The samples with the most exciting results were characterised by XPS and AES in order to assess the distribution of nickel and titanium in the materials passive films.

- The open circuit potential measurements have shown an enhancement of the passive behaviour of the alloys subjected to thermal treatments, with oxidation in N_2 environment providing more positive E_{corr} stable values. The potentiodynamic polarization curves illustrate a marked passive region for all samples, with the untreated NiTi presenting a higher current density at the passive region. This means that the thermal treatments provide a more protective character to the oxide film on NiTi's surface, in which relies its resistance to corrosion; among the four different treatments, the ones performed at higher tempera-

tures (350 °C) lead to the best corrosion performance.

- From the EIS results, the resistance to corrosion is extremely improved by oxidation at 350 °C in nitrogen atmosphere, with high and constant impedance values along the whole experiment. In the other modified alloys, the corrosion resistance is very high for t = 0h, but their passive layer starts to become less protective over time, with resistance decreasing in the order 350 °C air > 250 °C N_2 >> 250 °C air. The native NiTi's oxide film presents a very different behaviour: although starting with a low corrosion resistance, it increases over time. A "duplex" structure was proposed for the Nitinol passive oxide, composed by a dense inner layer and an outer porous one, leading to an equivalent circuit that fits the experimental data.

- The surface analysis results show different concentrations of nickel and titanium within the passive films, for untreated and treated NiTi at 350 °C. The spectrum demonstrate that the native film is quite thin, as proved by the presence of Ni and Ti in the metallic form (by XPS) and in an equiatomic proportion for relative low depths (seen in AES depth profile).
  The treatments conducted in two different environments brought different oxide films constitutions, with almost no presence of nickel in the outermost oxide layers obtained from oxidation in N_2 atmosphere; in this situation, the release of that element is minimized in case of corrosion.

- The selective oxidation of titanium over nickel is related with the low Gibbs free energy of TiO_2 in comparison to that of NiO. In this way, and in a situation of oxygen shortage, Ti will have higher tendency to form oxides than Ni, which will provoke an enrichment of the former species on the outermost layers of the passive film.
  With respect to the differences observed for oxidation at 250 and 350 °C, kinetic reasons can be invoked. Being the oxidation reaction closely dependent on the temperature, being accelerated with T increase, it is understandable to obtain thicker oxide layers for 350 °C, enhancing the material's protection.

- It is possible to conclude from this work that the performed thermal treatment in nitrogen environment at 350 °C brings undoubtedly improvements, in comparison with the native alloy, in terms of corrosion resistance and nickel content reduction at NiTi's surface, which can also be interpreted as a biocompatibility optimization. To get a more complete evaluation, a study of the mechanical and fatigue properties should be opportune, in order to understand the effects of the thermal oxidation at all levels, including in the transition temperatures.
  In fact, *in vivo* tests give a broader perspective of a device's performance, since it is conducted in a realistic environment, in which the material face dynamic conditions as it would naturally inside the human body.

- Since the thermal treatments at 250 °C did not bring considerable advantages, a suggestion for a future work would be to perform those treatments at a temperature closer to 300 °C and to check if the corrosion resistance is comparable with those treated at 350 °C; in theory, a thicker film, despite minimising the nickel release to the surrounding medium, might affect considerably the mechanical properties of the material, jeopardising its application. In principle, and in case of similar corrosion behaviours, alloys thermally treated at lower temperature may be better. To quantify the thickness of the formed oxide film, the observation of the material's cross-section by electron microscopy (SEM or TEM) would be an interesting choice.

References

[1] Ellingham diagrams. http://web.mit.edu/2.813/www/readings/Ellingham_diagrams.pdf. Last access on: 19-11-2016.

[2] V. V. Andreeva. Behavior and nature of thin oxide films on some metals in gaseous media and in electrolyte solutions. *Corrosion*, 20(2):35t–46t, 1964.

[3] M. Assad, L. H. Yahia, C. H. Rivard, and N. Lemieux. *In vitro* biocompatibility assessment of a nickle-titanium alloy using electron microscopy in situ end-labelling (emisel). *Journal of Biomedical Materials Research*, 41(1):154–161, 1998.

[4] F. Auricchio, E. Boatti, and M. Conti. Sma biomedical applications. In L. Lecce and A. Concilio, editors, *Shape Memory Alloy Engineering: for Aerospace, Structure and Biomedical Applications*, chapter 11, pages 307–341. Elsevier Ltd., 2015.

[5] M. Berger-Gorbet, B. Broxup, C. Rivard, and L. H. Yahia. Biocompatibility testing of niti screws using immunohistochemistry on sections containing metallic implants. *Journal of*

Biomedical Materials Research, 32(2):243–248, 1996.

[6] Q. Chen and G. A. Thouas. Metallic implant biomaterials. In *Materials Science and Engineering: R: Reports*, volume 87, pages 1–58. 2015.

[7] B. E. Conway. *Electrochemical Data*. Elsevier, 1952.

[8] A. U. Drago, S. Stanciu, R. Cimpoeu, I. Ionita, M. Raoi, T. Constantin, I. Cimpoeu, and M. Agop. The corrosion resistance of niti-active element before and after thermomechanical solicitation. *Applied Mechanics and Materials*, 371:353–357, 2013.

[9] N. C. A. Figueira. Caracterizao do comportamento face corroso da liga niti - qualidade em aplicaes biomdicas. Master's thesis, Instituto Superior Tcnico, 2008.

[10] A. Itro, V. Garau, G. P. Tartaro, and G. Colella. Experience with a rigid fixation device in maxillofacial surgery using shape-memory clips. *Minerva stomatologica*, 46(7–8):381–389, 1997.

[11] J. Izquierdo, M. B. Gonzlez-Marrero, M. Bozorg, B. M. Fernndez-Prez, H. C. Vasconcelos, J. J. Santana, and R. M. Souto. Multiscale electrochemical analysis of the corrosion of titanium and nitinol for implant applications. *Electrochimica Acta*, 203(10):366–378, 2016.

[12] E. J. Kassab and J. P. Gomes. Assessment of nickel titanium and beta titanium corrosion resistance behavior in fluoride and chloride environments. *Angle Orthodontist*, 83(5):864–869, 2013.

[13] K. Matsumoto, N. Tajima, and S. Kuwahara. Correction of scoliosis with shape-memory alloy. *Nihon Seikeigeka Gakkai Zasshi*, 67(4):267–274, 1993.

[14] A. Michiardi, C. Aparicio, J. A. Planell, and F. J. Gil. Electrochemical behaviour of oxidized niti shape memory alloys for biomedical applications. *Surface and Coatings Technology*, 201(14):6484–6488, 2007.

[15] J. Mieluch. Impedance methods in electrochemical investigations. *Corrosion Protect*, 3:78, 1990.

[16] F. L. Nie, Y. F. Zheng, Y. Cheng, S. C. Wei, and R. Z. Valiev. In vitro corrosion and cytotoxicity on microcrystalline, nanocrystalline and amorphous niti alloy fabricated by high pressure torsion. *Materials Letters*, 64(8):983–986, 2010.

[17] L. Petrini and F. Migliavacca. Biomedical applications of shape memory alloys. *Journal of Metallurgy*, 2011:1–15, 2011.

[18] S. A. Shabalovskaya, G. C. Rondelli, A. L. Undisz, J. W. Anderegg, T. D. Burleigh, and M. E. Rettenmayr. The electrochemical characteristics of native nitinol surfaces. *Biomaterials*, 30(22):3662–3671, 2009.

[19] L. L. Stepan, D. S. Levi, and G. P. Carman. A thin film nitinol heart valve. *Journal of Biomechanical Engineering*, 127(6):915–918, 2005.

[20] F. Takeshita, H. Takata, Y. Ayukawa, and T. Suetsugu. Histomorphometric analysis of the response of rat tibiae to shape memory alloy (nitinol). *Biomaterials*, 18(1):21–25, 1997.

[21] F. Villermaux, M. Tabrizian, L. Yahia, M. Meunier, and D. L. Piron. Excimer laser treatment of niti shape memory alloy biomaterials. *Applied Surface Science*, 109–110:62–66, 1997.

[22] Y. Yu, T. Sun, and Y. Wang. Bioactive titanium oxide coatings fabricated on niti sma via thermal treatment for medical applications. In *8th International Conference on Materials for Advanced Technologies*, volume 141, pages 115–120. MRS Singapore ICMAT Symposia Proceedings, 2016.

[23] J. X. Zhang, R. F. Guan, and X. P. Zhang. Synthesis and characterization of solgel hydroxyapatite coatings deposited on porous niti alloys. *Journal of Alloys and Compounds*, 519(13):4643–4648, 2011.